Fouling mitigation and wastewater decontamination in UV treatment systems

Fouling mitigation and wastewater decontamination in UV treatment systems

Tooba Aslam, Efthalia Chatzisymeon*

School of Engineering, Institute for Infrastructure and Environment, University of Edinburgh, Edinburgh EH9 3JL, UK.

*Corresponding author: e-mail: e.chatzisymeon@ed.ac.uk; tel.: 0044 1316505711

Abstract

This work applied the photo-Fenton process to mitigate quartz fouling in UVA wastewater treatment. The impacts of the pH, iron, and phosphorus concentration in synthetic wastewater were explored. It was observed that the photo-Fenton process (5 mg/L Fe^{2+}, 10 mg/L H_2O_2) mitigated quartz fouling and achieved 33% of chemical oxygen demand (COD) removal. It was also found that the presence of UVA irradiation and/or acidic conditions substantially decreased fouling formation. X-ray diffraction as well as energy-dispersive spectroscopy measurements showed that fouling consisted mainly of Fe, Ca, P and Na. Increasing P concentration in wastewater from 5 mg/L to 40 mg/L enhanced fouling formation as well as COD removal from 35% to 51%, respectively. This work provides insight, for the first time, into the role of Fenton processes in mitigating quartz fouling, one of the technical challenges in upscaling photocatalytic treatments.

Keywords: Advanced oxidation processes; photocatalysis; fouling mitigation; wastewater treatment

1. Introduction

Ultraviolet (UV) based technologies such as photolysis, photocatalysis and photo-Fenton treatment, are commonly applied for wastewater decontamination. These processes have recently received considerable attention mainly because of their effectiveness in degrading persistent priority and emerging contaminants from wastewater. These contaminants can remain untreated in conventional wastewater treatment plants (WWTPs), which were not initially designed to remove such persistent substances. Therefore, UV based technologies can be a promising tertiary treatment able to be incorporated in existing WWTPs. However, a major technical obstacle in UV based systems is quartz fouling (Blatchley et al., 1996). Quartz fouling is attributed to the deposit of suspended or dissolved particles on the surface of the quartz that houses the UV lamps. Based on the type of the material that is deposited onto the quartz surface, fouling can be divided into colloidal, organic, inorganic and biological. These fouling materials can absorb UV radiation, and therefore substantially decrease the performance of irradiation processes (Blatchley et al., 1996). Quartz is a hydrophobic surface that at near neutral or basic pH can provide active sites due to the dissociation of silanol groups on its surface. Several chemical reactions including adsorption, complexation and precipitation can take place on these active sites that eventually lead to fouling formation (Stumm, 1992). Important factors that can affect the formation of fouling include the physicochemical characteristics of wastewater (Watkinson, 1986; Watkinson and Martinez, 1975) such as the pH, colour, turbidity, taste, odour and hardness. For example, acidic pH can cause dissolution of metals (i.e., lead, copper, zinc etc.) leading towards precipitation or adsorption of these onto the organic matter present in the water. High turbidity, which is a measurement of the suspended inorganic matter, also leads towards the formation of fouling. Previous studies have been carried out to understand the effect of these factors on fouling formation during UV treatment (Nessim and Gehr, 2006) (Lin et al., 1999). Mitigation techniques for fouling formation have been also explored. For example, (Younis et al., 2018) proposed a UV disinfection system where UV lamps housed in quartz tubes are not in direct

contact with the water. The system consisted of a quartz tube through which the untreated water flowed and the UV lamps (1.5 W/cm^2) were located outside the quartz tube, which prevented the formation of biofilm and accumulation of mineral residues. They also studied the addition of ozone as an oxidant to reduce the chemical contaminants of water and therefore further reduce formation of fouling. Pre-treatment of wastewater have been also examined as a way to reduce fouling formation. A study conducted by (Ali et al., 2022) assessed the performance of a solar photocatalytic reactor (TiO_2/H_2O_2) as pre-treatment for wastewater to control membrane fouling. This increased the removal of turbidity and total organic carbon (TOC) from the final effluent. There have been many articles using photocatalysis as pre-treatment for wastewater to avoid fouling on membrane materials, but to the best of the author's knowledge, there are no studies examining the role of Fenton processes in mitigating fouling formation during photocatalytic treatment of wastewater.

Therefore, this work aims to deploy Fenton and photo-Fenton process to mitigate the formation of quartz fouling. Wastewater decontamination and how this can be affected by the presence of fouling, water pH, iron and phosphorus concentration were also studied. Changes of fouling formation on the surface of the quartz sleeves and reduction of organic matter in municipal wastewater was observed by microscopy techniques. Metal concentrations in the fouling cake and in wastewater were also measured.

2. Materials and methods

2.1 Materials

The synthesized wastewater comprised appropriate amounts of Fe^{2+} ($FeSO_4.7H_2O$; ≥99.0%, CAS No: 7782-63-0, Sigma Aldrich) and P (K_2HPO_4), 10 mg/L of $CaCl_2$ (96%, CAS No: 10043-52-4, Acros), 1 mg/L $MgCl_2.6H_2O$ (99+%, CAS No: 7791-18-6, Acros), 10 mg/L of humic acid (CAS No: 1415-93-6; Sigma Aldrich), 30 mg/L of urea (CAS No: 57-13-6, Fisher Scientific UK) and 110 mg/L of meat extract purchased from Sigma Aldrich. Its pH was 8.9. In order to

dissolve humic acid, 10 – 20 mL of 0.1 N NaOH was added to the solution. Deionised water was collected from Alto™ Ultrapure water system, Triple Red Ltd. H_2O_2 (CAS No: 7722-84-1) was also used.

2.2 Experimental runs

Experiments were carried out in photocatalytic batch reactors as shown in Figure 1. UVA irradiation was emitted by a 368 nm lamp with a power output of 11 W, which was housed in an immerse quartz cell. The synthetic wastewater in the reactors was continuously stirred (150 – 200 rpm) to achieve uniform mixing and to promote dispersion. Reactors were covered with parafilm to avoid evaporation. Experiments without UV irradiation were also performed. Water samples were taken regularly from the reactors and were analysed for metal concentrations, absorbance at 254 nm, and chemical oxygen demand (COD) content. Observations about fouling formation on the quartz surface were made on daily basis. All the experiments were conducted at room temperature. In order to check the effect of acidic pH and simulate photo-Fenton operational parameters experiments were performed at 2.8 pH by using 0.1 M HNO_3. Each experiment lasted for 5 days to allow time for fouling formation and growth.

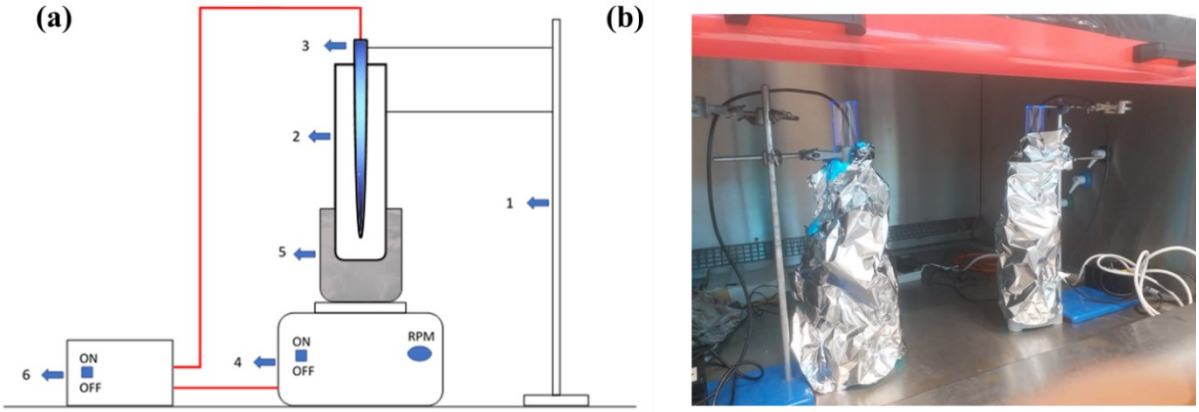

Figure 1: (a) Schematic drawing of the experimental setup with UVA: (1) clamp, (2) quartz sleeve, (3) UVA lamp, (4) magnetic stirrer, (5) reactor vessel, (6) DC power supply; (b) photo of the UV reactors in the lab.

2.3 Microscopy and analytical techniques

Photocatalytic performance was evaluated with respect to organic removal from wastewater by measuring its chemical oxygen demand (COD) according to the potassium dichromate standard method. A YSI 910 COD Colorimeter (YSI Xylem Analytics, UK), COD digestion tubes (Palintest PL450 (0-150 mg/L) or PL484 (0-1500 mg/L)), and a block heater (Hach 16500-10) were used for COD measurements. H_2O_2 was monitored by the peroxide test strips (1-100 mg/L H_2O_2) purchased from Fisher Scientific, UK. A WTW OXI340i Oxygen Meter with a compatible pH probe was used to measure the pH. A Cary 100 Scan UV-Vis Spectrophotometer (VARIAN) was used to measure wastewater's absorbance at 254 nm spectrum. Mg, P, Ca, and Fe concentration in water were analysed by 8900 Triple Quadrupole ICP-MS (Agilent with octopole reaction system) employing an RF power of 1550 W and RF Matching voltage of 1.8 V, with argon gas flows of 15 L/min, 0.9 L/min and 1.03 L/min for plasma, auxiliary and nebuliser flows, respectively. Transmittance was calculated by Equation (1) and measuring UV absorbance of the water samples at 254 nm:

$$\%T = \text{anti-log}\,(2-A) \qquad (1)$$

where T stands for transmittance and A for absorbance at 254 nm.

This formula indicates that if all the light passes through a clear solution without any absorption, then absorbance is zero and transmittance is 100%.

Scanning electron microscopy (SEM) images of the fouling cake were taken in a Carl Zeiss SIGMA HD VP Field Emission Scanning Electron Microscope with a Schottky thermal field emitter as the electron source, operated at 15 kV accelerating voltage using secondary imaging. SEM as well as energy dispersive spectroscopy (EDS) measurements were made using the same instrument and an Oxford Aztec Energy dispersive X-ray analysis system. For this analysis, samples were analysed as thin films on glass slides and coated with carbon to achieve a conductive surface.

2.4 Experimental matrix

Initial preliminary experiments were performed to assess the formation of fouling and suitability of the reactors and the main experiments are shown in Table 1.

Table 1. Experimental matrix for the treatment of synthetic wastewater by UV-based processes.

Experimental run	Fe, mg/L	P, mg/L	H_2O_2, mg/L	Water pH	Irradiation
1	5	5	-	8.9	-
2	10	5	-	8.9	-
3	20	5	-	8.9	-
4	40	5	-	8.9	-
5	5	5	-	2.8	-
6	10	5	-	2.8	-
7	20	5	-	2.8	-
8	40	5	-	2.8	-
9	5	5	-	2.8	UVA
10	10	5	-	2.8	UVA
11	20	5	-	2.8	UVA
12	40	5	-	2.8	UVA
13	5	5	-	2.8	-
14	5	10	-	2.8	-
15	5	20	-	2.8	-
16	5	40	-	2.8	-
17	5	5	-	2.8	UVA
18	5	10	-	2.8	UVA
19	5	20	-	2.8	UVA
20	5	40	-	2.8	UVA
21	5	5	-	2.8	-
22	5	5	-	2.8	UVA
23	5	5	5	2.8	UVA
24	5	5	10	2.8	UVA

3. Results and discussion

Experiments were performed to study the formation of fouling as well as the decontamination of wastewater during UVA treatment. As a preamble, it was concluded that fouling formation was substantially affected by the presence of either iron, phosphorous, H_2O_2 or their combinations in water. The effects of these parameters as well as of other operational parameters are discussed below.

3.1 The effect of iron concentration

3.1.1 Basic pH

The effect of wastewater's iron concentration on fouling formation was explored firstly at ambient pH 8.9 and without any artificial UVA irradiation (experiments 1 – 4 in Table 1). The amount of iron spiked in the reactors was 5 mg/L, 10 mg/L, 20 mg/L and 40 mg/L. The wastewater was left in the reactor for 5 days to assess fouling formation on the quartz sleeves and the results are shown in Figures 2 and 3. It can be observed that the amount of fouling attached onto the surface of the quartz is increased when the concentration of iron in the wastewater is increased. Also, the yellow-brownish colour gets darker and precipitates are increased with increasing the amount of iron (from 5 mg/L to 40 mg/L) in the water (Figure 2).

Figure 2: Fouling formation on quartz sleeves with synthetic wastewater at various iron (Fe^{2+} from $FeSO_4.7H_2O$) contents of 5 mg/L, 10 mg/L, 20 mg/L, 40 mg/L added in the reactor vessels

from left to right respectively. Turbidity increases with the increase in the concentration of Fe^{2+}. No source of light present. Basic pH.

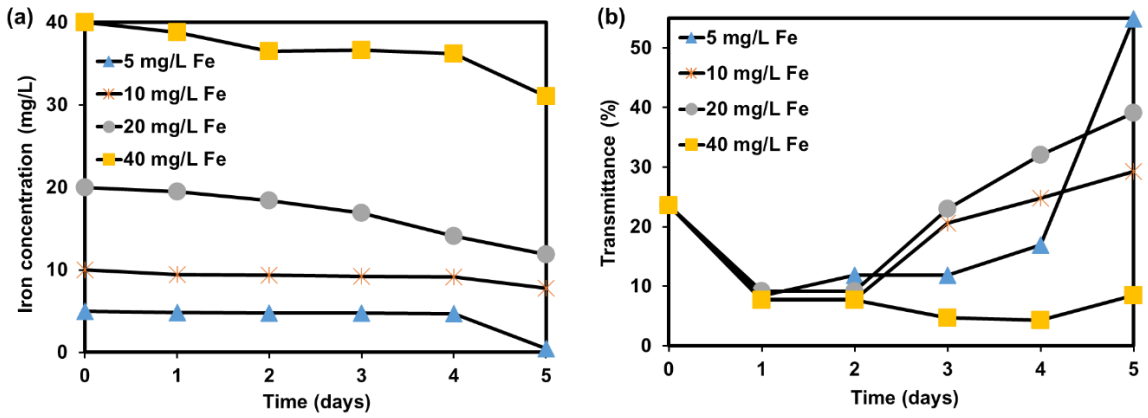

Figure 3: Effect of the water's dissolved iron (source: $FeSO_4.7H_2O$) content on the (a) iron concentration and (b) transmittance. Duration of the experiment is 5 days. Basic pH, without UVA.

Figure 3 shows iron concentration and wastewater transmittance during experiments 1 – 4. It was observed (Figure 3a) that the amount of iron content of the solution, is reduced by 91%, 22%, 41% and 22% in case of 5 mg/L, 10 mg/L, 20 mg/L and 40 mg/L of iron added respectively. This can be attributed to the basic conditions (pH ranges between 8 and 9), and implies that the iron precipitated out in the form of iron oxide and/or deposited on the quartz surface as iron-organic complexes. This could be also seen on the sleeves of quartz surface in Figure 2. This is consistent with results for wastewater transmittance (Figure 3b). After day 1 transmittance decreased from 23% to about 9% and then started to increase after the day 3 in the presence of all 5 mg/L, 10 mg/L and 20 mg/L iron. In the presence of 40 mg/L iron, transmittance decreases until day 4 and slightly increases after that. This can be attributed to the high amount of iron added in the wastewater that creates lots of flocs and precipitates, which can remain suspended in the water as there are not enough active sites on the quartz

surface, compared to the amount of suspended solids, therefore dragging the fouling formed to be re-suspended into the solution. This is also consistent with Figure 2 where it is shown that in the presence of 40 mg/L of Fe^{2+}, suspended solids are in the bulk volume of water as well as on the quartz surface. These results show that fouling growth can increase when there are increased iron amounts in water at ambient pH. According to literature, solubilisation and precipitation of iron depend on the pH of water (Rose et al., 1998). When basic conditions occur, ferrous iron (Fe^{+2}) can be rapidly oxidised in the presence of oxygen and more iron is complexed by hydroxide as suggested by (Theis and Singer, 1974; Saleh and Gupta, 2016). Previous studies conclude that formation of iron-organics and other cation-organics complexes is potentially of importance in the promotion of organic fouling and/or as a precursor of cationic accumulation in the foulant. As suggested by Tipping (1981) (Tipping, 1981), the dissolved magnesium (Mg^{+2}) and calcium (Ca^{+2}) are capable of increasing the capacity of iron oxides to absorb humic substances (co-adsorption of these cations) at basic pH which is quite the reason for the decrease in organics as measured by UV absorbance at 254 nm.

3.1.2 Acidic pH

Experiments 5 – 8 (shown in Table 1) at various iron concentrations were carried out in acidic conditions (pH 2.8) in which photo-Fenton oxidation reaction rates are optimal. Results are shown in Figure 4. It was observed visually that the amount of the fouling deposited on the quartz surface in this case is significantly lesser than in basic conditions discussed in section 3.1.1.

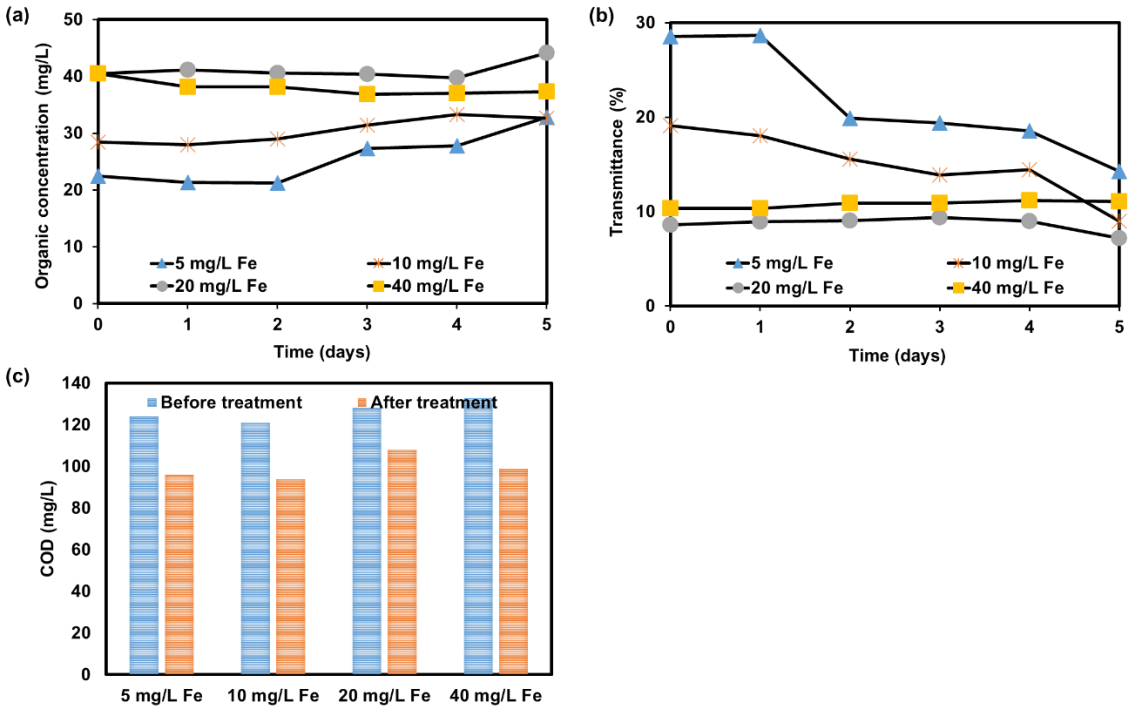

Figure 4. Effect of water's iron (source: $FeSO_4.7H_2O$) content on (a) organic concentration in mg/L measured by UV-Vis absorbance at 254 nm, (b) the water transmittance, and (c) the COD concentration. pH is 2.8, without UVA.

An increase in UV absorbance at 254 nm was observed (Figure 4a) in all cases after day 2 of treatment. According to previous studies, this behaviour could be attributed to the fact that at lower pH hydrolysis of substances can result in high UV absorbance (Saghezchi et al., 2008) Another reason could be the presence of ionic iron, nitrates and nitrites that have been reported to interfere with UV absorbance measurements. At the same time water transmittance is reduced (Figure 4b), thereby increasing the absorbance at 254 nm, and this could be also attributed to the precipitation of humic substances at pH lower than 2. These precipitated humic substances could be attached to the wall or accumulate at the bottom of the reactor reducing the transmittance of the water. However, it is expected that this slightly contributed to decreased transmittance in this set of the experiments because the pH always remained between 2.8 - 3. Transmittance was found to decrease by 35%, 53%, 16% and increased by 6% in case of 5 mg/L, 10 mg/L, 20 mg/L and 40 mg/L of iron, respectively (Figure

4b). Moreover, the iron content of the wastewater remained practically unchanged since it was reduced by 5%, 6%, 8% and 5% in case of 5 mg/L, 10 mg/L, 20 mg/L and 40 mg/L of iron, respectively (data not shown). Meanwhile, COD removal was about 17% for 5, 10, and 20 mg/L Fe^{2+} and increased to 23% COD removal at 40 mg/L Fe^{2+} at the end of treatment. This indicates that oxidation of ferrous to ferric ion takes place, but at slow reaction rate.

3.1.3 UVA treatment at acidic pH

Results from experiments 9 – 12 (shown in Table 1) were carried out to assess the effect of UVA irradiation and its role in fouling mitigation. The results are presented in Figure 5 and visual observations showed that there was no fouling formed on the quartz surface. The absence of fouling formation might be attributed to the fact that iron is soluble in acidic environments as ferrous ions remain soluble in water and no particles are deposited on the surface of the quartz (Pignatello et al., 2006). However, iron could be oxidised, even at slow rate, to ferric hydroxide in acid solutions, but this is not happening in the presence of UVA (raised temperature). The evaporation in this set of the experiment was 7-10% of the total volume. The initial hardness of the synthetic wastewater was 92.4 mg/L as $CaCO_3$ which increased to 99.0, 116.6, 121 and 158.4 mg/L $CaCO_3$ by the end of treatment at 5, 10, 20 and 40 mg/L of iron, respectively.

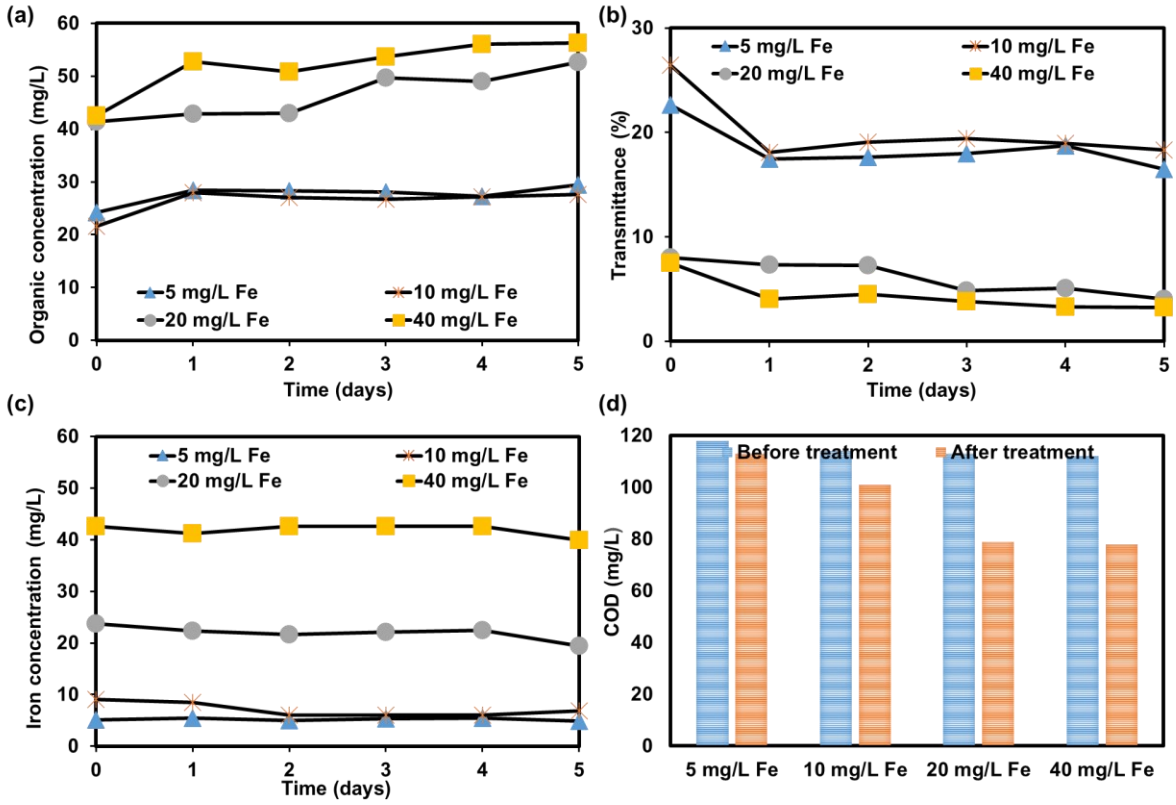

Figure 5: Effect of wastewater's iron content (source: $FeSO_4.7H_2O$) on (a) organic concentration in mg/L measured by UV-Vis absorbance at 254 nm, (b) wastewater transmittance, (c) iron concentration, (d) COD concentration. pH is 2.8, with UVA.

Similarly, to results shown in section 3.1.2, the wastewater transmittance is slightly decreased and UV absorbance at 254 nm is increased (Figures 5a and 5b). This could be attributed to the interferences caused by the ionic iron at 254 nm. COD is decreased by 4%, 11%, 30% and 30% in case of 5 mg/L, 10 mg/L, 20 mg/L and 40 mg/L of iron respectively (Figure 5d), which can be attributed to the presence of UVA irradiation that promotes the generation of hydroxyl radicals, though at low amounts. The production of HO radicals could be relatively enhanced by increasing the amount of iron to a reasonable level, for example at 20 mg/L Fe^{2+}, since it was observed that increasing the iron concentration from 10 mg/L to 20 mg/L increased COD removal from 11% to 30%. However, in case of 40 mg/L Fe^{2+}, the COD removal reaches plateau and remains at 30% as in the case of 20 mg/L Fe^{2+}. The reason behind this unchanged

COD removal percentage is that, at an increased amount of iron (source: $FeSO_4.7H_2O$), the solution might get saturated with Fe^{2+} and its solubility may start decreasing.

3.1.4 Fouling formation

To better understand the chemical and physical characteristics of the fouling cake, SEM and EDS measurements were made and the results are shown in Figure 6. The deposits were scrapped off the quartz surface with the help of a scrapper tool. The deposits that were not easily scrapable were extracted in a 0.1% HCl solution.

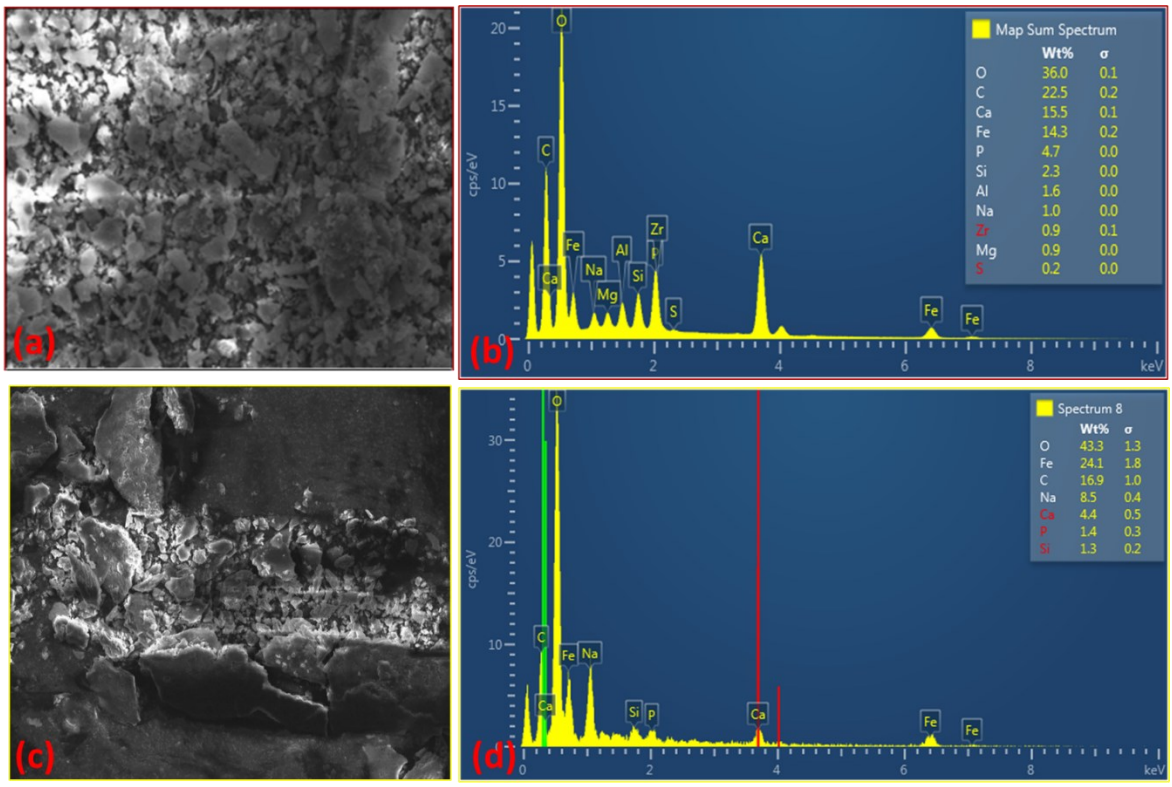

Figure 6. SEM and EDS measurements of the fouling formed after treatment at basic (ambient) pH (a) SEM image for 5 mg/L iron (Fe^{2+}) and with UVA lamp, (b) EDS spectrum for 5 mg/L iron (Fe^{2+}) and with UVA lamp, (c) SEM image with 5 mg/L iron (Fe^{2+}) and without UVA irradiation, (d) EDS spectrum with 5 mg/L of iron (Fe^{2+}) and without UVA lamp.

SEM images in the presence of UVA (Figure 6a) show a relatively homogeneous and dense structure of the crystals in the fouling cake while without UVA (Figure 6c), when the amount

of fouling is more, the structure becomes less homogeneous and more amorphous. EDS results in Figure 6b show that the major elements found in the foulant were C (22.5% wt), Ca (15.5% wt), Fe (14.3% wt), and P (4.7% wt). The foulant composition in the absence of UVA (Figure 6d), included Fe (24.1% wt), C (16.9% wt), Na (8.5% wt) and Ca (4.4% wt). In both cases Fe was among the most abundant metals in the foulant and this is consistent with the decrease of iron concentration in wastewater (Figure 3a). Also, Si was present in the foulants, which indicates the dissociation of the silane groups on the surface of the quartz that is responsible for initiating the fouling formation. Other elements such as Ca, Na and P are also found in the foulant which is in good agreement with previous studies (Nessim and Gehr, 2006; Lin et al., 1999). Most of the carbon (C) comes from the carbon stubs used to transport the sample to SEM.

3.2 Effect of phosphorous

As phosphorous is one of the major elements along with iron and calcium in fouling when analysed by XRD (EDS) in the previous experiments, the effect of phosphorous (Source: K_2HPO_4) concentration in wastewater, without UVA (runs 13 – 16 in Table 1) and with UVA irradiation (runs 17 – 20 in Table 1), on fouling growth and COD removal were studied. Experiments were performed using different amounts of phosphorus spanning from 5 mg/L, to 10 mg/L, to 20 mg/L and to 40 mg/L and results are shown in Figure 7. In the absence of UVA irradiation, evaporation was less than 10%, the temperature did not rise above 22 ^{o}C, and pH remained between 2.8-2.9 in all cases. The electrical conductivity was in the range of 0.86 - 1.0 mS/cm^2 throughout the experiment. In the presence of UVA irradiation, evaporation was less than 9% which might not have caused change in the concertation of wastewater constituents due to the change in the solvent volume. Temperature did not exceed 35 ^{o}C.

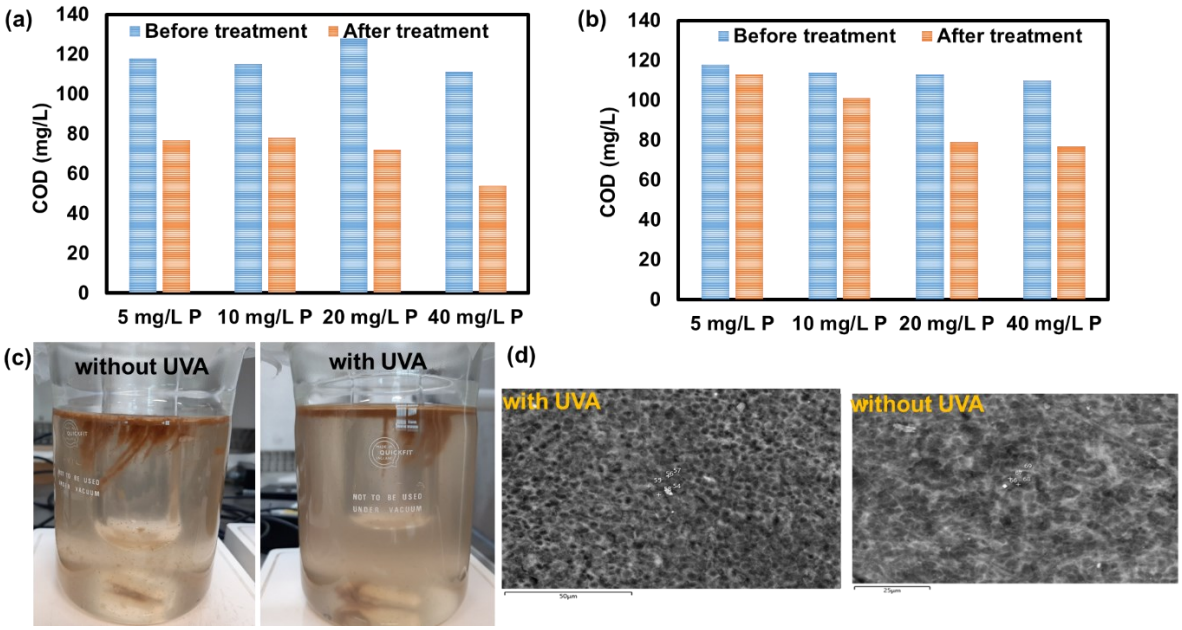

Figure 7. COD removal after 5 days of treatment at acidic pH (a) without UVA, and (b) with UVA irradiation. Before treatment refers to the COD (mg/L) at zero day with different concentrations of P. After treatment refers to the COD (mg/L) at the end of the 5 days. (c) Pictures of fouling formed on the surface of wastewater without (left) and with (right) UVA. (d) SEM images of fouling cake with and without UVA irradiation.

In Figure 7a COD was removed by 35%, 32%, 43% and 51% in the presence of 5 mg/L, 10 mg/L, 20 mg/L and 40 mg/L of phosphorus, therefore removal percentages were increased for P concentrations higher than 10 mg/L. This increase in COD removal may be attributed to the fact that ionic iron binds with the organic matter (soluble COD) and as a result it can sweep along part of soluble COD (Li, 2005). As can be seen in Figure 7c, the amount of the fouling formed in wastewater with and without UVA light, was quite significant. The reason behind this might be the increased hardness of water, which was 92.4 mg/L $CaCO_3$ in the initial synthetic wastewater and increased to 99, 116.6, 121, and 158.4 mg/L $CaCO_3$ in the presence of 5, 10, 20 and 40 mg/L of phosphorus, respectively. This is consistent with previous studies (Federation, 1996; Sheriff and Gehr, 2001). Another reason for the formation of this amount of fouling could be the adsorption of phosphate ion onto the iron and aluminium oxides due to

acidic conditions (Guppy et al., 2005). This might have led to ferric phosphate precipitation which happens below pH 3.5 at around 25 ºC. According to the literature, orthophosphate adsorbs to Fe oxy(hydroxide) minerals mainly by replacing hydroxyl groups present on mineral surfaces (Tejedor-Tejedor and Anderson, 1990; Arai and Sparks, 2001). These surface functional groups can also interact with carboxylic acids coming from humic substances (organic matter) that consist of oxygen-containing functional groups, such as carboxyl and hydroxyl groups which explains their interactions with Fe and P (Stevenson, 1994). This means that iron, phosphorus and organic matter could be bound together, which could also contribute to the increased COD removal. Moreover, in the presence of UVA irradiation (Figure 7b) COD removal rate was also found to increase when P concentration was increased from 5 mg/L to 40 mg/L. To be more specific, COD removal was 4%, 11%, 31% and 42% at 5 mg/L, 10 mg/L, 20 mg/L and 40 mg/L of phosphorus, respectively, which is less COD removal than without UV. Wastewater transmittance and phosphorus concentration remained almost unchanged during these experiments. SEM images of the fouling cake showed that its structure was quite homogeneous in both cases (with and without UVA irradiation) in Figure 7d. XRD measurements showed that the major elements in the fouling cake were P followed by Fe and K without UVA, and P followed by S, Fe and K in the presence of UVA. Both these results indicate that increased concentrations of P in the wastewater can significantly contribute to the formation of quartz fouling.

3.3 Effect of H_2O_2 concentration

H_2O_2 was added to the reactant solution to assess the effect of photo-Fenton oxidation in terms of COD removal and fouling formation. H_2O_2 was added at concentrations ranging from 5 mg/L to 10 mg/L (runs 21 – 24 in Table 1) and the results are shown in Figure 8.

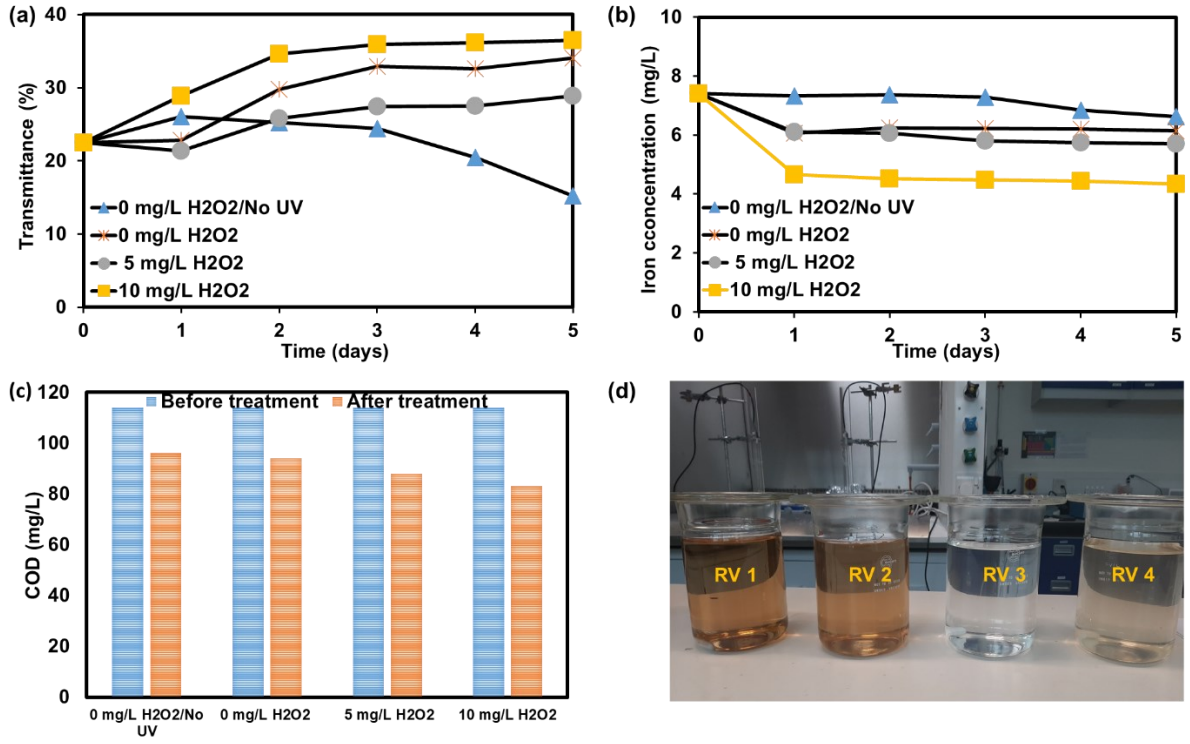

Figure 8. Photo-Fenton treatment and control experiments at 5 mg/L Fe^{2+} in synthetic wastewater. (a) effect on transmittance %, (b) effect on iron (Fe^{2+}) concentration, (c) COD removal. Before treatment refers to the COD (mg/L) at zero day with different concentrations of H_2O_2. After treatment refers to the COD (mg/L) at the end of the 5 days. (d) Pictures of the treated effluent (RV1: no H_2O_2/no UVA, RV2: no H_2O_2/UVA, RV3: 5mg/L H_2O_2/UVA, RV4: 10 mg/L H_2O_2/UVA).

COD removal was 28% and 33% in the presence of 5 mg/L and 10 mg/L H_2O_2 respectively (Figure 8c), which can be attributed to the fact that photo-Fenton (i.e. UV/H_2O_2/Fe) can enhance the oxidation potential especially of organics contaminants by promoting the generation of hydroxyl radicals in wastewater (Mierzwa et al., 2018; Ameta et al., 2013). On the other hand, lower COD removal was observed without hydrogen peroxide, in which cases (RV1 and RV2 in Figure 8d) the highest fouling formation was observed, probably because very low amounts of radicals were generated. Transmittance was decreased from 26% to 15% in RV1, where there was practically no treatment and that is why more fouling was observed

in this case. The iron concentration in wastewater is decreased by 40% in RV4 (i.e., with 10 mg/L of H_2O_2), which implies that the photo-Fenton reaction is taking place. Turbidity, COD, TSS, TDS of water were also decreased in RV4. Moreover, it can be observed that COD removal was also enhanced with the increase in H_2O_2 concentration which produces higher amount of hydroxyl radicals which can attack non-selectively more organic pollutants. This is the reason that COD removal is higher in the presence of 10 mg/L H_2O_2 than at 5 mg/L H_2O_2.

4. Conclusion

The formation of fouling and the decontamination of synthetic wastewater were studied during treatment by UVA photo-Fenton oxidation process. Operating factors like the pH, and the concentration of iron and phosphorus in wastewater were examined. Changes of fouling formation on quartz sleeves and COD removal were monitored during the experiments. Metal concentrations in the fouling cake and in wastewater were also measured. It was observed that quartz fouling was developed more under ambient pH (slightly basic) mainly due to precipitation of elements (e.g., Fe, Ca, P) found in wastewater. Fouling formation was decreased at acidic conditions and/or in the presence of UVA irradiation. Transmittance of the wastewater was also reduced which could be attributed to ferric and humic acid precipitation. The photo-Fenton treatment (i.e., addition of H_2O_2 along with iron under UVA light at acidic conditions) increased the overall efficiency of the system both in terms of decreasing fouling formation on quartz sleeves and increasing COD removal. Therefore, results from this work can be used to avoid quartz fouling during up-scaling of UV processes for water and wastewater treatment.

Acknowledgements

Funding was provided by the Higher Education Commission (HEC) of Pakistan. For the purpose of open access, the authors have applied a Creative Commons Attribution (CC BY) license to any Author Accepted Manuscript version arising from this submission. The data that support the findings of this study are available from the corresponding author upon reasonable request.

References

Ali, N. S., Kalash, K. R., Ahmed, A. N. & Albayati, T. M. 2022. Performance of a solar photocatalysis reactor as pretreatment for wastewater via UV, UV/TiO2, and UV/H2O2 to control membrane fouling. Scientific Reports, 12, 16782.

Ameta, R., Benjamin, S., Ameta, A. & Ameta, S. C. 2013. Photocatalytic degradation of organic pollutants: a review. Materials Science Forum, 734, 247-272.

Arai, Y. & Sparks, D. L. 2001. ATR–FTIR Spectroscopic Investigation on Phosphate Adsorption Mechanisms at the Ferrihydrite–Water Interface. Journal of Colloid and Interface Science, 241, 317-326.

Blatchley III, E. R., Bastian, K. C., Duggirala, R. K., Alleman, J. E., Moore, M. & Schuerch, P. 1996. Ultraviolet irradiation and chlorination/dechlorination for municipal wastewater disinfection: assessment of performance limitations. Water Environment Research, 68, 194-204.

Guppy, C., Menzies, N., Moody, P. & Blamey, F. P. C. 2005. Competitive sorption reactions between phosphorus and organic matter in soil: A review. Australian Journal of Soil Research, 43.

Li, J. 2005. Effects of Fe(III) on Floc Characteristics of Activated Sludge. Journal of Chemical Technology and Biotechnology, 80, 313-319.

Lin, L.-S., Johnston, C. T. & Blatchley, E. R. 1999. Inorganic fouling at quartz: water interfaces in ultraviolet photoreactors—I. Chemical characterization. Water Research, 33, 3321-3329.

Mierzwa, J. C., Rodrigues, R. & Teixeira, A. C. 2018. UV-hydrogen peroxide processes. Advanced oxidation processes for waste water treatment. In Emerging Green Chemical Technology, Academic Press. 13-48.

Nessim, Y. & Gehr, R. 2006. Fouling Mechanisms in a Laboratory-Scale UV Disinfection System. Water Environment Research, 78, 2311-2323.

Pignatello, J. J., Oliveros, E. & Mackay, A. 2006. Advanced oxidation processes for organic contaminant destruction based on the Fenton reaction and related chemistry. Critical reviews in environmental science and technology, 36, 1-84.

Rose, J., Vilge, A., Olivie-Lauquet, G., Masion, A., Frechou, C. & Bottero, J.-Y. 1998. Iron speciation in natural organic matter colloids. Colloids and Surfaces A: Physicochemical and Engineering Aspects, 136, 11-19.

Khosravi Saghezchi, M., Sarpoolaky, H., Heshmatpour., F., 2008. The influence of pH and UV visible absorbtion on hydrolysis stage and gel behaviour of glasses synthesised by sol-gel. Iranian Journal of Materials Science and Engineering, 5(2) 15-21.

Saleh, T. & Gupta, V. 2016. Membrane fouling and strategies for cleaning and fouling control. Nanomaterial and Polymer Membranes, 25-53.

Sheriff, M. & Gehr, M. 2001. Laboratory investigation of inorganic fouling of low pressure UV disinfection lamps. Water Quality Research Journal, 36, 71-92.

Stevenson, F. J. 1994. Humus chemistry: genesis, composition, reactions, John Wiley & Sons.

Stumm, W. 1992. Chemistry of the solid-water interface: processes at the mineral-water and particle-water interface in natural systems, John Wiley & Son Inc.

Tejedor-Tejedor, M. I. & Anderson, M. A. 1990. Protonation of phosphate on the surface of goethite as studied by CIR-FTIR and electrophoretic mobility. Langmuir; 6(3) 602-611.

Theis, T. L. & Singer, P. C. 1974. Complexation of iron (II) by organic matter and its effect on iron (II) oxygenation. Environmental Science & Technology, 8, 569-573.

Tipping, E. 1981. The adsorption of aquatic humic substances by iron oxides. Geochimica et cosmochimica acta, 45, 191-199.

Watkinson, A. 1986. Scaling of plain and externally finned heat exchanger tubes. Journal of heat transfer, 108, 147.

Watkinson, A. & Martinez, O. 1975. Scaling of heat exchanger tubes by calcium carbonate. ASME J. Heat Transfer, 97, 504-508.

Younis, B. A., Mahoney, L. & Palomo, N. 2018. A Novel System for Water disinfection with UV radiation. Water, 10.